

Investigation the Effects of Micro-Riblet Film on a Wing-in-Ground Effect

Alireza Heidarian¹, Hassan Ghassemi² and Pengfei Liu³

¹Department of Marine Engineering, Persian Gulf University, Boushehr, Iran

²Department of Maritime Engineering, Amirkabir University of Technology, Tehran, Iran

³Australian Maritime College, University of Tasmania, Locked bag 1395, Launceston, TAS 7250, Australia

³International School of Ocean Science and Engineering, Harbin Institute of Technology, Weihai, 264200, China

²gasemi@aut.ac.ir

Abstract– Engineering marvels have led to the design and build the wing-in-ground-effect (WIG) crafts to fill the gap between ships and aircraft as a new opportunity for transportation. One of the most significant issues in WIG crafts design is drag and lift force when the craft starting to plane. In this study, living nature has been used as an instrument to solve the mentioned problem. There are various ways in nature to reduce drag force in fluid flow, such as the evidence in the movements of fish, sharks and dolphins, the skin of fast-swimming sharks is covered by micro-riblets that assist them to move fast. In this research, by using Computational Fluid Dynamics software ANSYS CFX the effects of riblets on the wing in ground effect were examined. A Clark-Y wing was simulated in simulation software at various Reynolds number and drag and lift coefficients are captured. The results reveal that by using the riblets on the wings in the ground 7 % drag reduction and 6% increase in lift force can be achieved.

Keywords– WIG Craft, CFD Method, Clark-Y Wing, Riblet, Drag Reduction and Lift Growth

I. INTRODUCTION

The main motivation to design WIG crafts was based on filling the gap between aircraft and watercraft. WIG crafts have greater velocity than conventional boats and are more efficient than aeroplanes. The rate of fuel consumption in WIG crafts is much optimized in comparison with aircraft. This advantage makes the WIG craft to have long flight endurance. Ground effect heavily impacts on the behaviour of the flow around the wing and it can create a dynamic air cushion when the wing moves near the ground. From one side, moving near the surface causes the stagnation point shifts to lower side of the wing and consequently the great portion of the air disturbing over the wing. From the other side, the velocity of the air on the other side of the wing is diminished and it causes to enhance the pressure [1].

A considerable pressure will be produced at the pressure side of the wing when the wing is moving in a very low ground clearance which this pressure called ram pressure. Simultaneously, the velocity of the downwash decreases and it leads to the reduction in produced drag [2]. Two theorems affect the aerodynamic characteristics of the wing when the wing nears the ground. These are called span dominated and chord dominated ground effect. The main parameter regarding

the wing in ground effect is ground clearance which considered as h/c (height/ chord ratio) [3]. Many researchers have made some efforts to develop WIG crafts to fly near the ground. Russia, Finland, Sweden and the United States were the pioneer in the design and build of high-speed WIG crafts. Nowadays, many countries have started to design this crafts Because of the efficiency and many merits of them compared to water and air craft [4].

The studies on the configuration of WIG crafts experimentally and theoretically have been made to improve their aerodynamic performance. Ram effect is the principal measure to extend lift force; when the flow exists under the wing around the stagnation point on the lower surface of body is trapped [2]. The gathering of high pressure on the lower surface and low pressure on the upper surface of the body produces a high lifting force which increases the source of support. Chun and Chang numerically investigated the turbulent flow of the wing with and without considering the effects of the ground [5]. An incompressible Reynolds Average Navier-Stokes (RANS) equation with finite difference method was applied in their numerical model. According to their computational results, the type of ground model does not have much effect on the lift and moment coefficients, but influence on the predicted drag coefficients. In another research which was done by Zerihan and Zhang the pressure and wake distribution around the wing were analyzed and were validated by experimental test [6].

For 2D simulation with the structured mesh A Reynolds-averaged Navier–Stokes (RANS) was employed and the SST $k-w$ and Saplart-Allmaras turbulence models were applied to investigate the flow around the wing. Telenta et al demonstrated that SST $k-w$ and realizable $k-\varepsilon$ turbulence models are suitable for estimating the pressure distributions and visualization of wake region, respectively. They used multi-block hybrid grids. Also, the standard $k-\varepsilon$ turbulence model was applied for a racing car wing [7]. The flow considerably accelerates as the wing approaches with proximity to the ground which results in higher suction and consequently greater downforce as compared with free stream since the flow around the wing is bound up by ground clearance. The greater downforce may lead to the separation of the fluid at the rear of suction surface. There are different ways to overcome separation effects in aircraft; one of the

applicable methods is using micro-riblet film. The high velocity of sharks motivates the scientists to study the skin of fast sharks. They found that the skin of them are covered with micro-riblet film and they can control the flow pattern around themselves and it helps them to move more easily in the water and riblets influence on the viscous sublayer and flow pattern [8].

Using shark's riblets is deemed to be a better solution to destroy the effects of the separation on the wing in the ground effect [9]. The skin of fast sharks is covered with small denticles which called riblet. The various geometries of the riblets are shown in Fig. 1. When the dominated drag is concluded by turbulent flow, using micro-riblets is a beneficial method for drag reduction goals [10]. In the objects which the main drag parameter is pressure drag, using of the riblets for drag reduction is not effective [11].

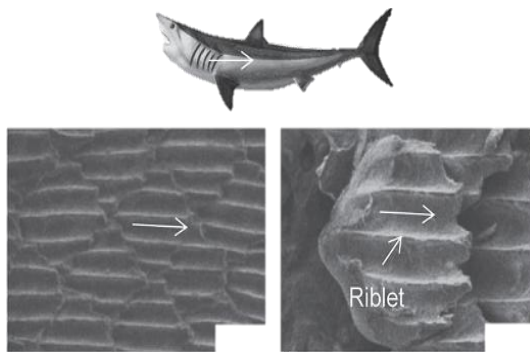
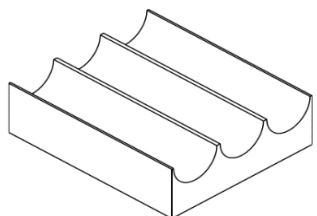


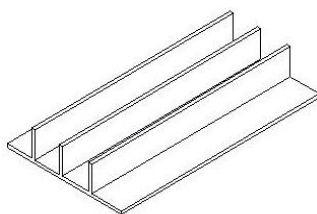
Fig. 1. Arrangement of riblets in fluid flow [12]

II. DRAG REDUCTION BY SHARK'S RIBLET

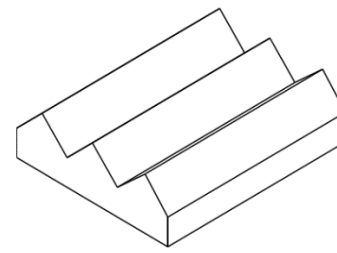
The skin of fast swimming sharks has been studied for drag reduction capabilities and it is shown that they are useful for responding to the pressure fluctuations across the surface [13]. The various geometries of shark's riblets such as scalloped, blade and sawtooth are given in Fig. 2 [14].



Scalloped Riblet



Blade Riblet



Sawtooth Riblet

Fig. 2. Different types of riblet [15]

In turbulent fluid flow, the existence of cross-flow velocity will cause a dramatic increase in momentum transfer [16]. Since the momentum transfer occurs parallel to the surface of the wing it increases the induced drag which caused by vortices. Riblets influence on turbulent flow pattern by decreasing the momentum transfer. This is possible by impress on two essential parameters, first is the elevation of the vortices above the surface and the second is the prevention of the creation the cross-stream velocity which leads to stream-wise vortices [15]. Although the application of riblet for drag reduction goals does not appear reasonable at the first glance, since riblets enhance the wetted area, thus it may cause increase the drag [17]. The main effect of the riblets is shifting the induced vortices to the tips of riblets and they reduce the interaction between surface and fluid flow since just the small area of the tips are encountered to flow and the fluid flow with greater shear stress occurs in this small surfaces whereas the vast domain and moderate speed has lower effects on the tips [18].

Therefore, the shear stress and momentum transfer is lower near a ribletted aerofoil, which reduces the effect of increased area due to the riblets [19]. To explain the reasons for efficiency of riblets it is interesting to note that the main effect of riblets is on the induced vortices. When the surface is covered by the micro-riblets the vortices have been shifted from the surface to peaks of the riblets [20]. Consequently, only small area of the peaks of the riblets encountered with high-velocity flow and induced vortices so ribletted aerofoil has lower shear stress and accordingly drag force.

III. NUMERICAL ANALYSIS

A simulation was done using the ANSYS design modeller software [21]. The computational geometry is shown in Fig. 3. A Clark-Y aerofoil was used which has a chord length of 7.5 cm and a span of 10 cm. In this study, the aerofoil was simulated by micro-riblet film and without micro-riblet. The aerofoil was placed in a fluid flow at various velocities. The size of the riblets that used in the ANSYS CFX simulation is $h = 162\mu m$, $s = 340\mu m$ and are given in Fig. 4. For 5 different velocities, principal aerodynamic characteristics were compared between the plain (no riblet) and ribletted aerofoil. Fig. 3 shows the physical domain of simulation. To simulate ground effects, the bottom wall is set to move with the inlet surface.

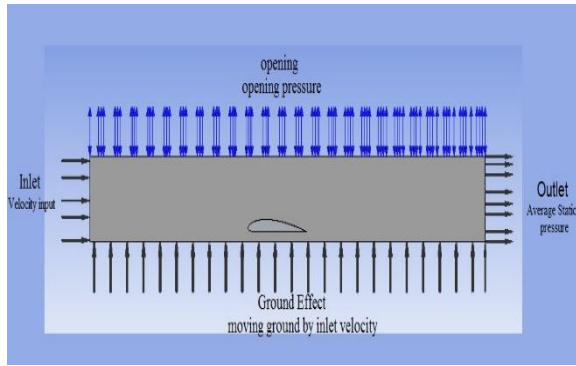


Fig. 3. Domain of simulation in ANSYS CFX

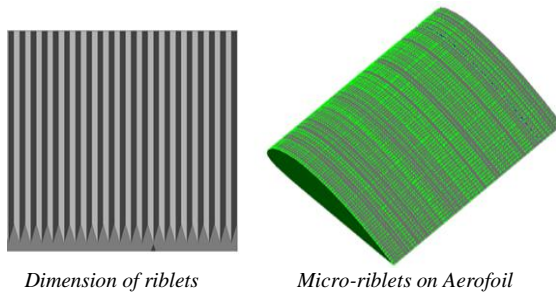


Fig. 4. The riblet size applied on aerofoil's surface

A) Meshing

A simulation was done by various number of mesh elements and eventually the optimum value of mesh is selected based on y^+ values. Five different meshes representing coarse (850,214 nodes), medium (2,053,680 nodes), fine (4,238,573), very fine (7,464,312 nodes) and ultrafine (10,464,312) Based on the maximum y^+ were checked to choose the desired mesh size and predicted drag coefficient. Considering Table I, the drag coefficient varies from coarse mesh to ultrafine mesh where an acceptable maximum $y^+ = 18$ is acquired. This value confirms that the boundary layer was reasonably well resolved. An inflation was set around the aerofoil and the volume of mesh was changed. By using 7.4 million nodes the predicted drag coefficient reached 0.211902 and after introducing the inflation by the first layer height of $5e-4$, about 10 million elements were acquired and the predicted drag coefficient reached 0. 21119 (less than 0.5 percent variation). Hence, in this simulation, the very fine mesh was chosen.

Table I. Different meshes examined for the riblets

Mesh	Nodes	Max y^+	Drag coefficient
Coarse	850,214	315	0.58031
Medium	2,053,680	158	0.31606
Fine	4,238,573	103	0.24779
Very Fine	7,464,312	56	0.211902
Extreme Fine	10,464,312	18	0. 21119

IV. RESULT AND DISCUSSION

In this study, the values of drag coefficient for ribletted aerofoil and plain aerofoil are calculated at different Reynolds number. Based on Fig. 5 the values of drag coefficient based on Reynolds number for the ribletted aerofoil is lower than plain aerofoil which it can admit the efficiency of the using riblets. Fig. 5 shows that by increasing the speed, the drag coefficient is reduced and the proportion of drag reduction are based on the Reynolds number. The maximum amount of drag reduction for ribletted aerofoil in comparison with the plain aerofoil is about 7%.

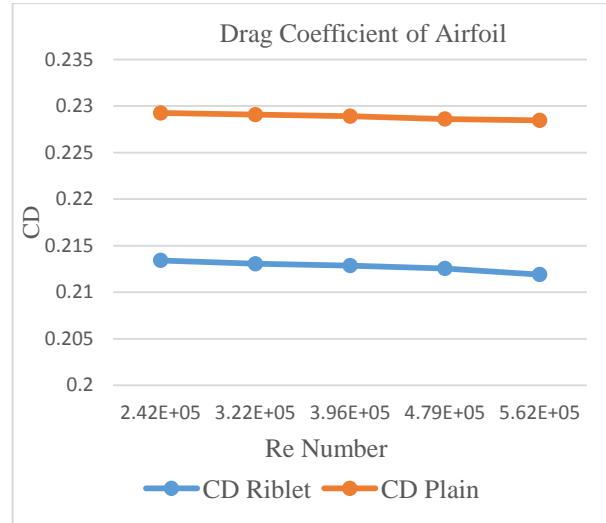


Fig. 5. Drag coefficient based on the Reynolds number for the plain and riblet aerofoils at different velocities

Another essential aerodynamics parameter which is calculated in this study is Lift coefficient. The values of lift coefficient are calculated in various Reynolds number.

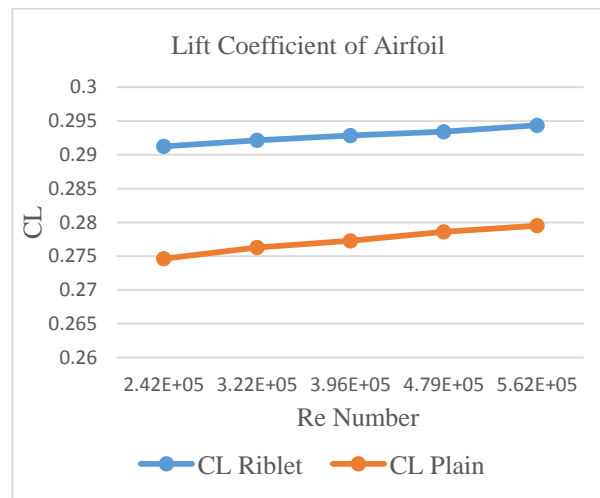


Fig. 6. Lift coefficient on the Reynolds number plain and riblet aerofoil at different velocities

Based on Fig. 6, the lift coefficient of the ribleted aerofoil is higher than the plain aerofoil in different velocities and it is because of the effects of riblets on induced vortices around the aerofoil. The riblets have some strong effects on the lift production due to vortices.

A) Pressure coefficient

The variation of the pressure coefficient (C_p) at the middle span of the rectangular wing was investigated in the ground effect and is shown in Fig. 7. The positive pressure on the lower surface and negative pressure (suction effect) on the upper surface of the wing increased when the micro-riblets are used.

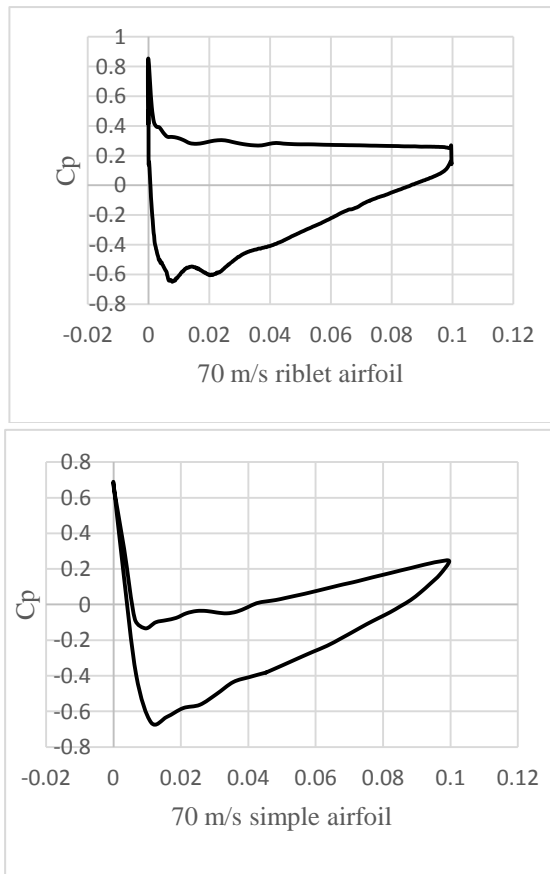


Fig. 7. Pressure coefficient along the chord of the midsection of the riblet and plain aerofoils

The pressure of the upper surface is lower than the lower surface. According to Fig. 7 at 70m/s, in the ribleted aerofoil created suction is higher than the plain aerofoil; consequently, higher suction pressure helps aerofoil to start planning easily so it leads to less fuel consumption. The flow considerably accelerates as the riblets applied on the aerofoil which results in a higher suction and therefore it may lead to greater downforce in comparison with free stream. Based on Fig. 7 the pressure difference between the upper and the lower surface of the ribleted aerofoil is higher than the plain aerofoil and it means that the ribleted aerofoil produced more lift force than the plain aerofoil.

B) Pressure Plots

Pressure contours in Fig. 8 represent that at various velocities the pressure difference of the plain aerofoil is smaller than ribleted aerofoil.

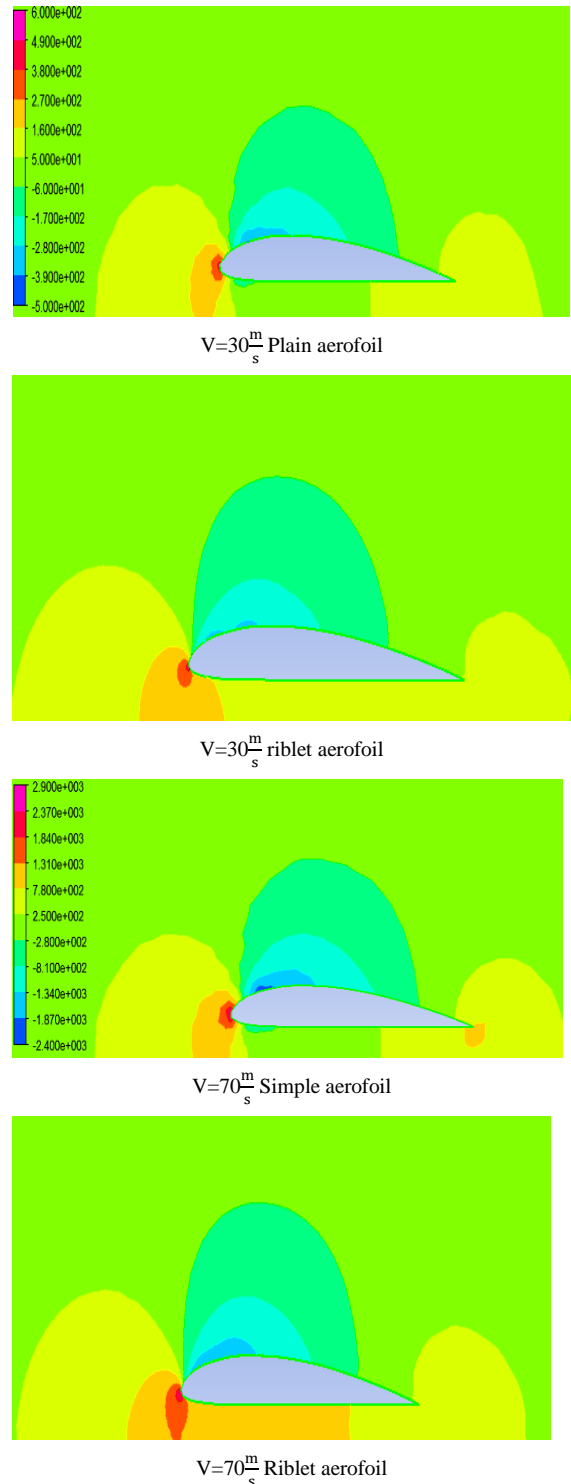


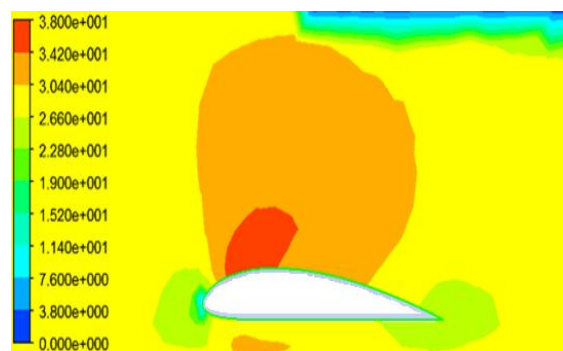
Fig. 8. Pressure contours for different velocities

While pressure starts to increase, the wing can easily start to plane because the air pressure helps it to fly, but in the

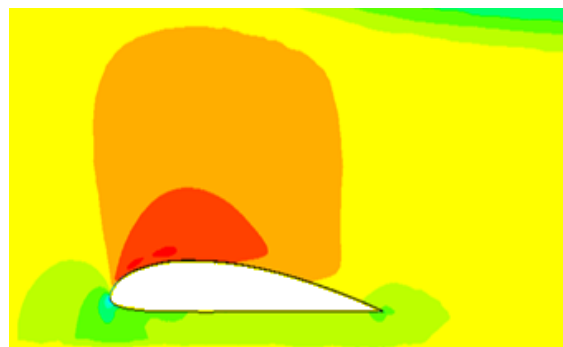
plain aerofoil, there is no auxiliary force and need higher energy to start flying. Consequently craft use plain aerofoil would need an engine of larger power and thus it would increase the cost of production of the aircraft and higher operation cost. For the ribletted aerofoil the stagnation point would be placed at the lower position than plain aerofoil and therefore the sensitive areas of the wing, especially at the leading edge of the aerofoil receives lower force than that of the plain aerofoil.

C) Velocity plots

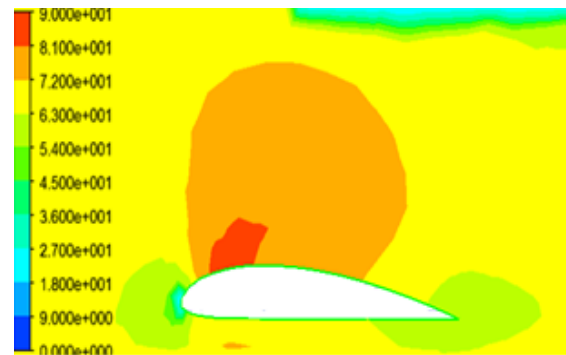
Velocity contours of ribletted aerofoil and plain aerofoil are shown in Fig. 9. Based on the figure, the separation on the ribletted aerofoil is delayed compared to the plain aerofoil. It means that the major parts of aerofoil have smaller pressure and the force due to the reduction of fluid separation and lift force are increased at similar velocities. The bottom of the ribletted aerofoil has smaller velocity and thus higher pressure compared with that of the plain aerofoil. The velocity contours in Fig 9 show that the occurrence probability of the separation in plain aerofoil is more likely than ribletted aerofoil. Based on Fig 9 the major area of the wing has smaller pressure and the force due to fluid separation drops and the lift force increases in similar velocities. In some aerofoils, the separation occurs near the leading edge so it provides an opportunity to produce bubbles which these bubbles can be dangerous especially towards the trailing edge where the flow is not reattached.



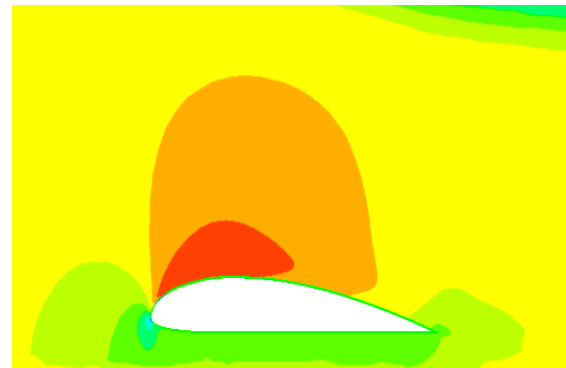
$V=30\frac{m}{s}$ plain aerofoil



$V=30\frac{m}{s}$ Ribletted aerofoil



$V=70\frac{m}{s}$ Plain aerofoil



$V=70\frac{m}{s}$ Ribletted aerofoil

Fig. 9. Velocity contours of different velocities for riblet and plain aerofoils

In this condition, the short bubbles and vortices can be merged and may result in a stall. Using micro-riblet film makes the flow to be more aberrant. Turbulent flow has more energy and momentum than laminar flow and hence it may eliminate separation and the flow may reattach. A short bubble may not be of much concern. The bottom of the ribletted wing has a lower velocity in comparison with the plain aerofoil. The separation in the boundary layer may lead to an enhancement of the displacement thickness which lessens the potential of fluid flow.

V. VALIDATION

NASA air craft results have revealed that by using micro-riblets can achieve 8 to 10% drag reduction and lift enhancement [22], [23]. The acquired results from our study and simulation and the results which obtained by NASA by applying 3M company riblets at various conditions are presented in Table II. The result of the simulation in CFX was completely checked with the presented results of the experiments. The modelled riblets were chosen to be the same size as the ones that were tested. The simulation was verified and produced a good agreement with the previous experimental measurements.

Table II. The comparison between Maximum drag reduction of present study and other experimental tests

Fluid	Riblet Design	Maximum Drag Reduction	Ref
Oil	Blade Riblet	9.9%	[24]
Air	Sawtooth	8%	[25]
Air	Sawtooth	8%	[26]
Air	Sawtooth	7%	Present Study

VI. CONCLUSIONS

One of the most important parameters in aviation industry and design of aircraft is drag reduction and fuel consumption which it can affect the environment and consequently influence the cost of operation. One promising way to decrease skin friction is to structure surfaces with riblets. This research numerically investigated the effects of shark's riblets on aerodynamics parameters of the aerofoil in air, for different Reynolds numbers. In this research, ANSYS CFX software is employed to simulate the effects of riblets on the physics of flow around the wing in ground effect at various velocities. Based on the results, shark's riblets can reduce the frictional drag in turbulent fluid flow dramatically. Riblets by affecting on vortices decrease shear stress and momentum transfer and consequently lead to drag reduction. The obtained results from CFD simulation software were examined by experimental data which were done by 3M Company riblets. Based on the predicted results, ribletted aerofoil has a higher drag reduction of about 7% aerofoil. By comparing the drag coefficients of the plain and ribletted flat plates it is concluded that riblets can reduce drag force about 7% and increase lift production of force about 6%. The recorded positive pressure on the lower surface of the ribletted wing was noticeably stronger than that of the plain wing.

REFERENCES

- [1]. Abdel Wahab, M., et al., *Experimental and Numerical Investigation of Flutter Phenomenon of an Aircraft Wing (Naca 0012)*. Mechanics, 2017. 23(4).
- [2]. Yang, W., Z. Yang, and C. Ying, *Effects of design parameters on longitudinal static stability for WIG craft*. International Journal of Aerodynamics, 2010. 1(1): p. 97-113.
- [3]. Jia, Q., W. Yang, and Z. Yang, *Numerical study on aerodynamics of banked wing in ground effect*. International Journal of Naval Architecture and Ocean Engineering, 2016. 8(2): p. 209-217.
- [4]. Qu, Q., et al., *Numerical study of the aerodynamics of a NACA 4412 airfoil in dynamic ground effect*. Aerospace Science and Technology, 2014. 38: p. 56-63.
- [5]. Jung, J.H., et al., *Mean flow characteristics of two-dimensional wings in ground effect*. International Journal of Naval Architecture and Ocean Engineering, 2012. 4(2): p. 151-161.
- [6]. Zerihan, J. and X. Zhang, *A single element wing in ground effect - Comparisons of experiments and computation*, in *39th*

- Aerospace Sciences Meeting and Exhibit*. 2001, American Institute of Aeronautics and Astronautics.
- [7]. Telenta, M., et al., *Detached Eddy Simulation of the flow around a simplified vehicle sheltered by wind barrier in transient yaw crosswind*. Mechanics, 2015. 21(3).
- [8]. Viswanath, P.R., *Aircraft viscous drag reduction using riblets*. Progress in Aerospace Sciences, 2002. 38(6): p. 571-600.
- [9]. Lee, S.J. and Y.G. Jang, *Control of flow around a NACA 0012 airfoil with a micro-riblet film*. Journal of Fluids and Structures, 2005. 20(5): p. 659-672.
- [10]. Bechert, D.W., et al., *Fluid Mechanics of Biological Surfaces and their Technological Application*. Naturwissenschaften, 2000. 87(4): p. 157-171.
- [11]. Dean, B. and B. Bhushan, *Shark-skin surfaces for fluid-drag reduction in turbulent flow: a review*. Philosophical Transactions of the Royal Society of London A: Mathematical, Physical and Engineering Sciences, 2010. 368(1929): p. 4775-4806.
- [12]. Brian Dean, B.B., *SHARK-SKIN SURFACES FOR FLUID-DRAG REDUCTION IN TURBULENT FLOW: A REVIEW*. Advances in Mechanics, 2012. 42(6): p. 821-836.
- [13]. Davies, C. and P.W. Carpenter, *Instabilities in a plane channel flow between compliant walls*. Journal of Fluid Mechanics, 1997. 352: p. 205-243.
- [14]. Zhao, D., et al., *Study on the Hydrophobic Property of Shark-Skin-Inspired Micro-Riblets*. Journal of Bionic Engineering, 2014. 11(2): p. 296-302.
- [15]. Bixler, G.D. and B. Bhushan, *Biofouling: lessons from nature*. Philosophical Transactions of the Royal Society of London A: Mathematical, Physical and Engineering Sciences, 2012. 370 (1967): p. 2381-2417.
- [16]. Heidarian, A., H. Ghassemi, and P. Liu, *Numerical Aerodynamic of the Rectangular Wing Concerning to Ground Effect*. American Journal of Mechanical Engineering, 2018. 6(2): p. 43-47.
- [17]. Matin, A., N. Merah, and A. Ibrahim, *Superhydrophobic and self-cleaning surfaces prepared from a commercial silane using a single-step drop-coating method*. Progress in Organic Coatings, 2016. 99(Supplement C): p. 322-329.
- [18]. A. Heidarian, Hassan.Ghassemi., P. Liu., *Numerical Analysis of the Effects of Riblets on Drag Reduction of a Flat Plate*. Journal of Applied Fluid Mechanics, 2018. 11(3): p. 679-688.
- [19]. Goldstein, D., R. Handler, and L. Sirovich, *Direct numerical simulation of turbulent flow over a modeled riblet covered surface*. Journal of Fluid Mechanics, 1995. 302: p. 333-376.
- [20]. Shelley, S.R., et al., *Fluid mobility over corrugated surfaces in the Stokes regime*. Physics of Fluids, 2016. 28(8): p. 083101.
- [21]. ANSYS CFX-Solver Theory Guide. 2011.
- [22]. Harvey, W.D., International Pacific Air and Space Technology Conference, Melbourne, Australia, Nov. 13-17, 1987, Proceedings (A89-10627 01-01). Warrendale, PA, Society of Automotive Engineers, Inc., 1988, p. 287-311., Jan 01, 1988.
- [23]. www.3Mworldlywise.co.uk.
- [24]. Bechert, D., et al., *Biological surfaces and their technological application - Laboratory and flight experiments on drag reduction and separation control*, in *28th Fluid Dynamics Conference*. 1997, American Institute of Aeronautics and Astronautics.
- [25]. Bechert, D.W., et al., *Experiments on drag-reducing surfaces and their optimization with an adjustable geometry*. Journal of Fluid Mechanics, 1997. 338: p. 59-87.
- [26]. Davies, C. and P.W. Carpenter, *Numerical simulation of the evolution of Tollmien-Schlichting waves over finite compliant panels*. Journal of Fluid Mechanics, 1997. 335: p. 361-392.